TISSUE ENGINEERING
Volume 13, Number 5, 2007

DOI: 10.1089/ten.2006.0338

Assessment of an Automated Bioreactor to Propagate and Harvest Keratinocytes for Fabrication of Engineered Skin Substitutes

BALAJI KALYANARAMAN, M.B., B.S.,[1] and STEVEN BOYCE, Ph.D.[2,3]

ABSTRACT

Engineered skin substitutes (ESS) composed of autologous fibroblasts and keratinocytes attached to collagen-glycosaminoglycan (GAG) scaffolds are effective adjuncts in the treatment of massive burns. The Kerator, an automated bioreactor for keratinocyte culture, could hypothetically reduce labor and material requirements, and increase availability of ESS. Human keratinocytes were cultured in the Kerator and also in tissue-culture flasks. It was found that keratinocyte confluence increased exponentially with time in both the Kerator ($r^2 = 0.99$) and the flasks ($r^2 = 0.96$). Confluence (mean ± SEM) of keratinocytes in the flasks (28 ± 2.3%) was significantly higher than in the Kerator (18 ± 0.93%) at day 4. However, there was no difference in confluence at harvest. The colony forming efficiency (CFE) and population doublings (PD) per day of keratinocytes harvested from the Kerator were 67 ± 4.7% and 0.80 ± 0.06, respectively, and were not different from the corresponding values for keratinocytes from flasks. ESS fabricated with keratinocytes from the Kerator or from the flasks were comparable *in vitro* in terms of histological anatomy, cellular viability, and surface hydration. These findings show that there are no differences between keratinocytes from the Kerator and those from the flasks regarding (a) growth to confluence, (b) CFE and growth rate (PD/day), or (c) quality of ESS *in vitro*, suggesting that the Kerator can automate fabrication of ESS and increase its availability for treatment of skin wounds.

INTRODUCTION

BIOREACTORS HAVE BEEN DEFINED as devices in which environmental and operating conditions can be closely monitored and tightly controlled to permit or induce desired biological and/or biochemical processes.[1] Bioreactors have been employed in the field of tissue engineering to perform one or more of the following functions: cell expansion,[2–7] generation of three-dimensional tissues from dissociated cells and scaffolds *in vitro*,[8–12] and mechanical conditioning of developing tissue.[13–15] The use of bioreactors facilitates scale-up of tissue-engineering bioprocesses,[2,3,5,7] automation of culture,[3,4] and improvements in the quality of engineered tissue.[13–16]

Skin is among the first tissues to be engineered *in vitro* and to demonstrate clinical efficacy.[17,18] The most significant use of tissue-engineered skin substitutes has been in the treatment of massive burns, where their application has resulted in early wound coverage, reduced harvesting of donor sites for autograft, and less scarring, thereby reducing morbidity and mortality.[17,19] Skin substitutes have also been used in the treatment of chronic ulcers and giant nevi.[20,21] The prospect of delivering gene therapy for somatic gene disorders through skin substitutes is being explored.[22,23] Apart from their clinical uses, skin substitutes have been employed in the pharmaceutical industry for toxicology assays, which has major implications for reduction in the number of animal subjects used in safety testing. Engineered

[1]Department of Biomedical Engineering, University of Cincinnati, Cincinnati, Ohio.
[2]Departments of Surgery and Biomedical Engineering, University of Cincinnati, Cincinnati, Ohio.
[3]Department of Research, Shriners Burns Hospital, Cincinnati, Ohio.

skin substitutes (ESS) are composed of an epidermal substitute of cultured human keratinocytes, and a dermal substitute of a bovine collagen-glycosaminoglycan (GAG) sponge populated with cultured human fibroblasts. ESS composed of autologous cells have been used clinically as effective adjuncts to autograft in the treatment of massive burns. Generation of ESS from a patient's skin biopsy involves isolation of keratinocytes and fibroblasts by means of primary culture, multifold expansion of the cells *in vitro* by means of serial passaging, serial inoculation of fibroblasts and keratinocytes on collagen-GAG sponge, and maturation of the ESS at the air-liquid interface before transplantation to the patient.[24] Completion of these complex procedures in a timely manner may impact directly the availability of ESS to patients with emergent medical needs.

The current methods of cell culture in flasks are extremely laborious and material-intensive, both of which contribute significantly to limited availability and high cost of the device. A bioreactor system such as the Kerator,[25–28] in which medium changes are automated and the reactor chamber is reusable, may hypothetically reduce both the labor and materials involved in cell expansion for ESS and thereby increase its availability to patients at reduced costs. The Kerator has a closed system to avoid microbial contamination, a disposable substrate for keratinocyte adhesion and proliferation, and a reusable, sterilizable reactor chamber. The image acquisition system of the Kerator allows visualization of living cells by video microscopy so that the culture can be harvested when an appropriate cell density has been reached. Earlier studies with the Kerator focused on the generation of an autologous wound dressing composed of confluent and sub-confluent epidermal keratinocytes.[27] In serum-free culture medium, the rate of keratinocyte proliferation on the fluorinated ethylene propylene (FEP) culture substrate of the Kerator was comparable to that on standard tissue-culture polystyrene.[25] The image acquisition system of the Kerator was validated for online monitoring of keratinocyte proliferation within the bioreactor.[25] These studies have shown that the Kerator bioreactor can support automated culture of keratinocytes. However, to use the Kerator for the fabrication of ESS, cultured keratinocytes must be harvested from the bioreactor to be inoculated on the fibroblast-populated collagen sponge. In conventional cell culture, harvesting of keratinocytes involves application of mechanical force (e.g., gentle tapping of flasks) to completely release the cells from the culture surface following trypsinization. Preliminary studies of keratinocyte harvest from the Kerator showed such procedures to be impractical because of the size and weight of the culture module. The earlier studies also demonstrated that prolonged exposure to trypsin (greater than 10 min) was required to detach keratinocytes from the substrate, but this resulted in sub-optimal clonogenic potential of the cells in the subsequent passage. It was observed that treating keratinocytes with 0.02% ethylenediamine tetra-acetic acid (EDTA) eliminated the need for prolonged trypsinization and the requirement for mechanical forces to harvest keratinocytes from the Kerator. The aims of this study were to compare the Kerator to flasks for percent confluence of cells during culture; viability of keratinocytes harvested, by determining colony forming efficiency (CFE) and population doublings (PD) rate; and the quality of ESS fabricated with keratinocytes harvested, by studying histological organization, cell viability, and epidermal maturation *in vitro.*

MATERIALS AND METHODS

Kerator bioreactor

The Kerator bioreactor, described in detail in earlier publications,[25–28] was used in this study with a slight modification (Fig. 1). Briefly said, the Kerator comprises a modular growth chamber that is connected to the reservoirs for fresh medium, cell suspension, and effluent medium by means of sterile silicone tubing. The growth chamber consists of parallel polycarbonate plates separated by polycarbonate spacers fitted with silicone O-rings. A layer of hydrophilic fluoroethylene polymer film (FEP C-20, DuPont, Wilmington, DE) covers the upper surface of each polycarbonate plate and provides the substrate for keratinocyte attachment and proliferation. The FEP film is transparent, gas permeable, and autoclavable. The surface area for cell growth of a single polycarbonate plate covered with FEP film is 630 cm^2. Five such plates can be stacked at a time in the growth chamber, yielding a cumulative growth area of 3150 cm^2. The polycarbonate spacer has ports for medium inlet, gas inlet, and gas outlet. The spacer has two concentric grooves for silicone O-rings, which helps to hold the FEP film in place and also provides a leak-proof seal. Two rigid aluminum frames, one each at the top and bottom, hold the polycarbonate plates and spacers together by means of threaded screws. After assembly, the growth chamber is leak-proof to both liquid and gas. The entirechamber can be dismantled after a round of cell culture, reassembled with new FEP film, and sterilized by autoclaving.

Medium and cells are transferred to and from the growth chamber by means of a bidirectional, multichannel peristaltic pump (Fig. 2). Pneumatic pinch valves regulate the flow of medium through the appropriate conduits for specific procedures. The growth chamber sits on a platform, which can be rocked back and forth by a pneumatic actuator to ensure equal distribution of medium and cells. A mass flow controller upstream of the growth chamber mixes air and 100% carbon dioxide (CO_2) to provide 5% CO_2 in air. This gas mixture is humidified and filtered before it enters the growth chamber. The air outlet of the growth chamber is connected to a CO_2 detector (Poytron IR CO_2, Draeger Safety, Pittsburgh, PA), and the reading from the detector is used to manually regulate the CO_2 concentration in the growth chamber at 5%.

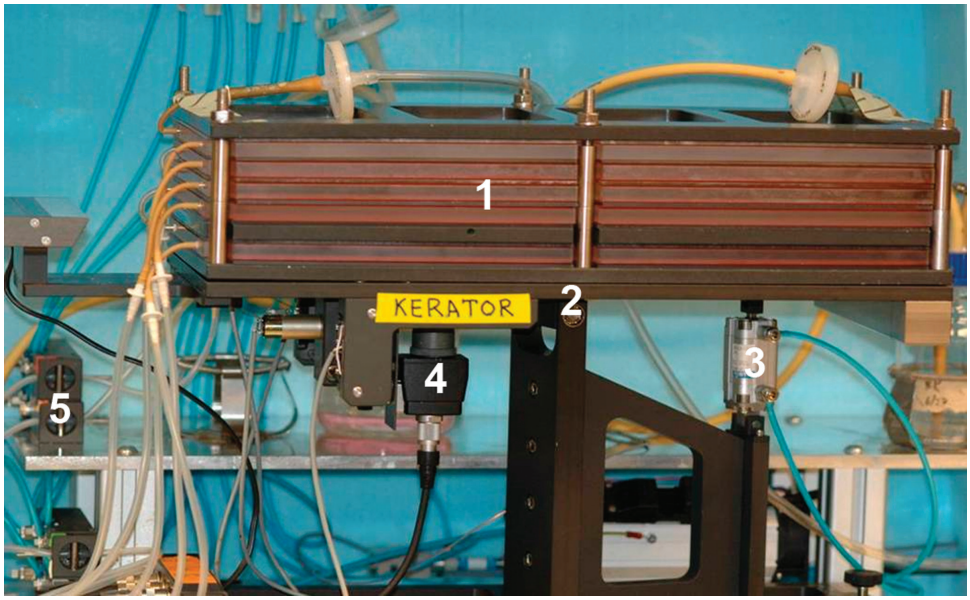

FIG. 1. Image of the growth chamber of Kerator bioreactor, showing (1) Five-layered growth chamber, (2) Rocking platform, (3) Pneumatic actuator, (4) Camera, and (5) Pneumatic pinch valves. Color images available online at www.liebertpub.com/ten.

The growth chamber sits inside an insulated box maintained at a temperature of 37°C using a hot plate and a thermostat.

The peristaltic pump, pinch valves, and the pneumatic actuator are controlled by the PC using the LabVIEW 6.1 Virtual Instruments (VIs) (National Instruments, Austin, TX). The VI provides a graphical user interface (GUI), by means of which culture parameters, namely, culture duration, frequency of medium change, volume of medium per medium change, and number of tilts of the rocking platform, can be regulated.

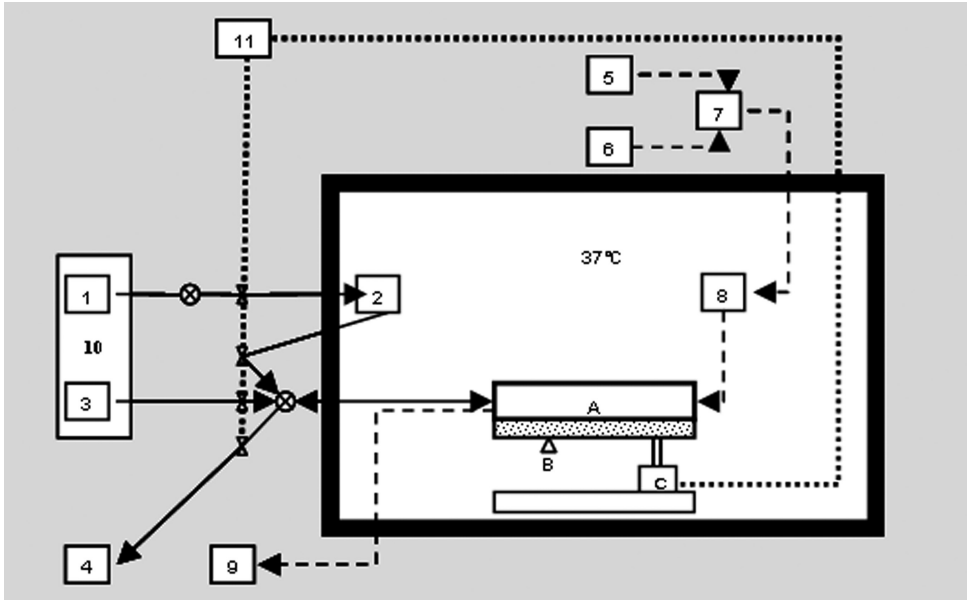

FIG. 2. Schematic representation of the Kerator. (A) Growth chamber, (B) Camera, (C) Tilting actuator, (1) Cold medium reservoir, (2) Warm medium reservoir, (3) Cell seeding and collection reservoir, (4) Waste, (5) CO_2 supply, (6) Air supply, (7) Mass flow controller, (8) Humidifier bottle, (9) CO_2 detector, (10) Peltier cooler, and (11) Compressed air supply.

Generation of a LabVIEW code for controlling the operations of the Kerator

LabVIEW 6.1 is a graphical programming language developed by National Instruments. In the case of the Kerator, there is a unidirectional flow of information from the LabVIEW code to the hardware components, which directs the operation of the culture system. For this purpose, input variables of the culture system need to be correlated to the output of the LabVIEW code so as to provide predictable and efficient control of the Kerator by the computer. The bidirectional peristaltic pump was first calibrated to determine the equation for flow rate (in mL/min). From known values for the flow rate (mL/min), and the rated speed of pump (rpm), equation 1 below was used to determine the constants for the slope (A) and the y-intercept (B).

$$\text{Flow rate (mL/min)} = A\ (\text{rated speed of pump}) + B \quad (1)$$

Then, for a predetermined volume x mL, the time output (y min) for which the pump had to be operated was calculated as

$$y = \frac{x}{A(rated\ speed) + B} \quad (2)$$

Thus, by inputting volume parameters for various aspects of culture (chamber washing, seeding, medium change), output values in terms of time were generated and used to control the Kerator. These values, along with the parameters for frequency of medium changes, number of tilts of the rocking platform, and time between successive tilts, were combined using specialized LabVIEW structures such as "For Loop," "While Loop," and "Sequence Structures" to generate a code for automated operation of the Kerator during keratinocyte culture.[29]

Image acquisition in the Kerator

A unique feature of the Kerator bioreactor is the image acquisition system that allows for visualization of keratinocytes in the lowest layer during the growth period. A 0.3 mega-pixel CCD camera lens is mounted onto the tilting platform mentioned above. By means of stepper motors, the camera can be moved horizontally to visualize different fields and vertically to adjust focus. The camera interfaces with the NI PCI 1411 (National Instruments) image acquisition board in the computer, and digital images are acquired and displayed using the IMAQ Vision Builder software (National Instruments). This imaging system allows visualization of keratinocytes growing within the Kerator in real time and helps in determining the time of harvest.

Keratinocyte culture in the Kerator

Cryopreserved normal human keratinocytes (NHK) derived from primary culture of surgical discard skin (from abdominoplasty) were expanded in T-flasks until sub-confluent and then harvested. Two strains of keratinocytes, CK 710 and CK 705, were used in the study. Keratinocytes in P2 (CK 710) or P3 (CK 705) were inoculated in the Kerator at a density of $4\times10^3/cm^2$. A parallel culture was established in T-225 cm^2 flasks at the same density to serve as control. Five T-25 cm^2 flasks were inoculated with the keratinocytes of the same passage at a density of 500 cells/cm^2 to determine CFE. Modified MCDB 153 supplemented with insulin, hydrocortisone, epidermal growth factor, 0.4% bovine pituitary extract, and antimicrobials (penicillin, streptomycin, and fungizone) was used as the culture medium and was changed manually every 2 days in the flasks. The Kerator was programmed to perform medium changes automatically every 48 hours. All experiments were repeated in triplicate.

Comparison of growth rate of keratinocytes between Kerator and flasks using image analysis

Using the imaging acquisition system in the Kerator described above, digital images of the proliferating keratinocytes were taken every 2 days beginning from the second day in culture to the end of culture ($n = 15$ images at each time point). Digital images of keratinocytes proliferating in T-225 flasks were taken at corresponding time points ($n = 15$ at each time point) using a 6 mega-pixel Nikon D70 camera mounted on a Nikon Diaphot phase-contrast microscope at 4× magnification and were used as controls. Using the image analysis software IMAQ Vision Builder (National Instruments) the images from the Kerator and the tissue-culture flasks were analyzed for the confluence of keratinocyte colonies as follows. The grayscale image was converted to a binary image by cell-edge detection followed by manual thresholding to remove noise. The binary image so created had a pixel value of 1 for cell-covered areas and 0 for empty areas in the image. By totaling the areas that had a pixel value of 1 in the binary image and expressing it as a percentage of the total pixel area of that image, the confluence value was obtained ($n = 6$).

Keratinocyte harvest from the Kerator

On day 7 of culture, keratinocytes were harvested from the Kerator in a semi-automated manner with the growth chamber *in situ*. After draining medium from the growth chamber and washing briefly (15 seconds) with Hepes buffered saline (HBS), the keratinocytes were incubated with 0.02% EDTA in HBS for 8 to 10 min. Following this step, the cells were incubated for 2–3 min with 0.025% trypsin-0.01% EDTA solution (15 mL/layer of growth chamber). When the cells were released from the culture surface, as visualized by the image acquisition system, the trypsin was neutralized by 10% fetal bovine serum and the resultant suspension was collected in the cell seeding/collection reservoir (numbered 3 in Fig. 2) by rinsing the chamber twice with HBS. All steps in the harvesting

process were performed in an automated manner by a custom LabVIEW VI, except neutralization of trypsin, which had to be initiated by the operator.

After collection, the cell suspension was centrifuged and the cells were resuspended in modified MCDB 153. The harvested keratinocytes were counted using a hemacytometer and were used to inoculate growth assays and ESS.

Keratinocyte harvest from tissue-culture flasks

After 7 days of culture, half of the flasks inoculated in parallel with the Kerator were harvested by brief (15–30 seconds) washing with HBS followed by treatment with 0.025% trypsin −0.01% EDTA for 5–6 min. This was the standard protocol used in this laboratory for harvesting keratinocytes. The remaining flasks were harvested using the same protocol as used for keratinocyte harvest from Kerator (hereafter referred to as flasks + EDTA), to control the modification of harvesting protocol in the Kerator. For each condition, the harvested cells were used to inoculate growth assays and ESS.

Growth assay of keratinocytes harvested from flasks and the Kerator

Five T-25 flasks each were inoculated with keratinocytes harvested from the Kerator and from flasks with keratinocytes inoculated at a density of 500/cm^2, and were used for determining CFE. After 4 days of culture, the keratinocytes in T-25 flasks were washed with HBS, fixed in 2% glutaraldehyde, and stained with 0.1% crystal violet. Digital images of the stained cells were taken under a phase-contrast microscope at 4× magnification (10 fields per flask, 50 fields per condition). The images were transferred to a computer where image analysis software (IMAQ Vision Builder) was used to count the number of colonies composed of four cells or more. From this, the CFE of keratinocytes was calculated using the following formulae[30] ($n = 6$):

$$\text{Number of colonies/cm}^2 = \frac{\text{Number of colonies per microscope field} \times 100}{\text{Area of a microscope field (mm}^2\text{)}} \quad (3)$$

$$\text{Colony forming efficiency(\%)} = \frac{\text{Number of colonies/cm}^2}{500\,\text{cells/cm}^2} \times 100\% \quad (4)$$

Three T-75 flasks each were inoculated with keratinocytes harvested from Kerator and from flasks with keratinocyte inoculation density of 4×10^3/cm^2, and were harvested after 7 days of culture. The resultant cell yield was used to calculate the growth rate of keratinocytes, in PD per day, using the following formulae[30]:

$$\text{Total number of population doublings} = \log_2\left\{\frac{(\text{Number of cells harvested} - \text{Colony incompetent cells})}{\text{Number of colony forming units}}\right\} \quad (5)$$

Wherein, Number of colony forming units = Number of cells inoculated × CFE

Colony incompetent cells = Number of cells inoculated × {100 − CFE}

$$\text{Growth rate} = \frac{\text{Total number of population doublings}}{\text{Culture period (days)}} \quad (6)$$

ESS fabrication and quality analysis in vitro

ESS ($n = 9$ per condition) were fabricated using type I bovine collagen sponge as scaffold material. Paired NHK and normal human fibroblasts (NHF) from two cell strains (705 and 710) were used to inoculate the ESS. NHF were recovered from cryopreservation, expanded in supplemented Dulbecco's modified Eagle's medium (DMEM), harvested, and inoculated on the collagen sponge at a density of 5×10^5/cm^2. The day after fibroblast inoculation, keratinocytes were harvested from Kerator and inoculated at a density of 1×10^6/cm^2. The following day, ESS were lifted to the air-liquid interface to allow for the maturation of stratum corneum and were cultured in that fashion for 21 days at 37°C in an atmosphere of 5% CO_2. UCMC 160 medium was used for the first 3 days of ESS incubation, and UCMC 161 medium was used from day 4 to the end of culture. Keratinocytes harvested from the T-225 flasks mentioned above were used to fabricate ESS in a similar manner and served as controls.

On days 7, 14, and 21 following keratinocyte inoculation, samples were taken from test and control ESS for histological analysis. The samples were paraffin-embedded, stained with hematoxylin and eosin (H&E), and viewed under the bright-field microscope for cellularity, epithelial organization, and maturation.

On days 7, 14, and 21 following keratinocyte inoculation, samples were taken from test and control ESS for 3-(4, 5-Dimethylthiazol-2-yl)-2,5-diphenyl tetrazolium bromide (MTT) assay.[31] This is a colorimetric assay for cellular viability that depends on the ability of mitochondria to cleave the tetrazolium salt MTT to formazan. The reaction product is solubilized by 2-methoxy-ethanol and can be read colorimetrically at 590 nm. At each time point, four 6 mm punch biopsies each were collected from test and control ESS and incubated in 0.5 mg/mL MTT solution for 3 hours at 37°C in an atmosphere of 5% CO_2. After 3 hours, 2-methoxy-ethanol was added to the samples and incubated for an additional 3 hours on a rocking platform. Following this step, the reaction product was measured in terms of the absorbance at 590 nm using a plate reader. MTT conversion for each ESS was expressed as the mean of four measurements at each time point.

On days 7, 11, 14, and 21 following keratinocyte inoculation, surface electrical capacitance (SEC) of the ESS was measured by using the impedance based Nova™ Dermal Phase Meter (DPM 9003; NOVA Technology Corporation, Gloucester, MA).[32] At each time point mentioned above, continuous SEC reading for 10 seconds was taken from five different locations in each ESS from the test and control conditions and was expressed in DPM units. The SEC for each ESS was expressed as the mean of the five readings taken at each time point.

STATISTICAL ANALYSES

The data for keratinocyte confluence, colony forming efficiency and growth rate, and MTT and SEC were expressed as mean ± standard error of the mean (SEM). The data were analyzed for statistical significance by one-way repeated measures (RM) analysis of variance (ANOVA), and significance was established at the 95% confidence level. Student-Neuman-Keuls test was used for pair-wise comparison following one-way RM ANOVA. All statistical analyses were done using the SigmaStat 3.0 software.

RESULTS

Confluence of keratinocytes in Kerator and flasks

Keratinocyte confluence was measured from digital images of cells on days 2, 4, and 6 of culture (Fig. 3). The digital images (Fig. 3A, C) were converted into binary images by thresholding for cell-covered regions of the image. The pixel area of cell-covered regions in the binary image was expressed as a percentage of total pixel area of the image to calculate the confluence, using the IMAQ Vision Builder software. In both the Kerator and the flasks, keratinocytes showed an exponential increase in confluence between days 2 and 6, with r^2 values of 0.99 and 0.96 for the Kerator and flasks, respectively (Fig. 4). Keratinocyte confluence in the Kerator on culture days 2, 4, and 6 were $6.4 \pm 0.97\%$, $18 \pm 0.93\%$, and $54 \pm 1.5\%$, respectively. At the corresponding time points, the confluences of keratinocytes in flasks were $8.7 \pm 1.6\%$, $28 \pm 2.3\%$, and $56 \pm 1.4\%$, respectively. The confluence of keratinocytes in Kerator was significantly lower than that in flasks on day 4 of culture ($p < 0.05$). There were no significant differences in keratinocyte confluence among the conditions on days 2 and 6 of culture.

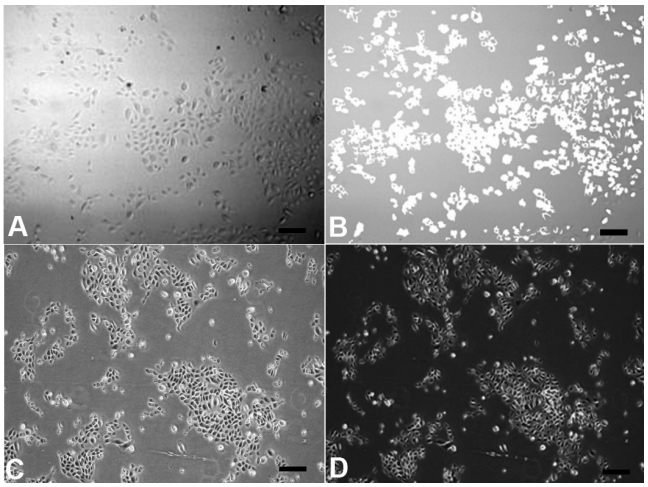

FIG. 3. Phase-contrast images of proliferating keratinocytes in Kerator (**A**) and flasks (**C**) on the fourth day of culture. The digital images were converted into binary images (**B, D**) by edge detection followed by thresholding to remove noise. Confluence of keratinocytes was calculated from the binary image by dividing the cell-covered area of the image (in white) with the total area of the image, in pixels. Scale bar = 100 μm.

Growth assay of keratinocytes following harvest from the Kerator

The CFE of keratinocytes harvested from the Kerator was $67 \pm 4.7\%$ (Fig. 5A). The CFE of keratinocytes

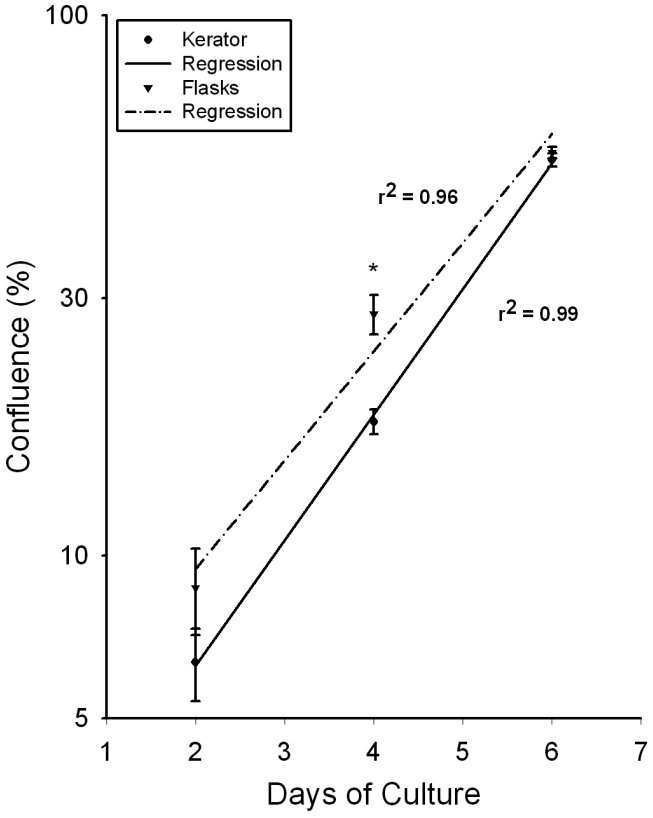

FIG. 4. Keratinocyte confluence in Kerator and flasks plotted as a function of time. Correlation values (r^2) indicate an exponential increase in keratinocyte confluence over time in culture in both conditions. The keratinocytes in flasks are significantly more confluent than those in the Kerator on the fourth day of culture as indicated by the asterisk ($p < 0.05$), but there is no significant difference in keratinocyte confluence between the two conditions on days 2 and 6 of culture. Error bars represent SEM.

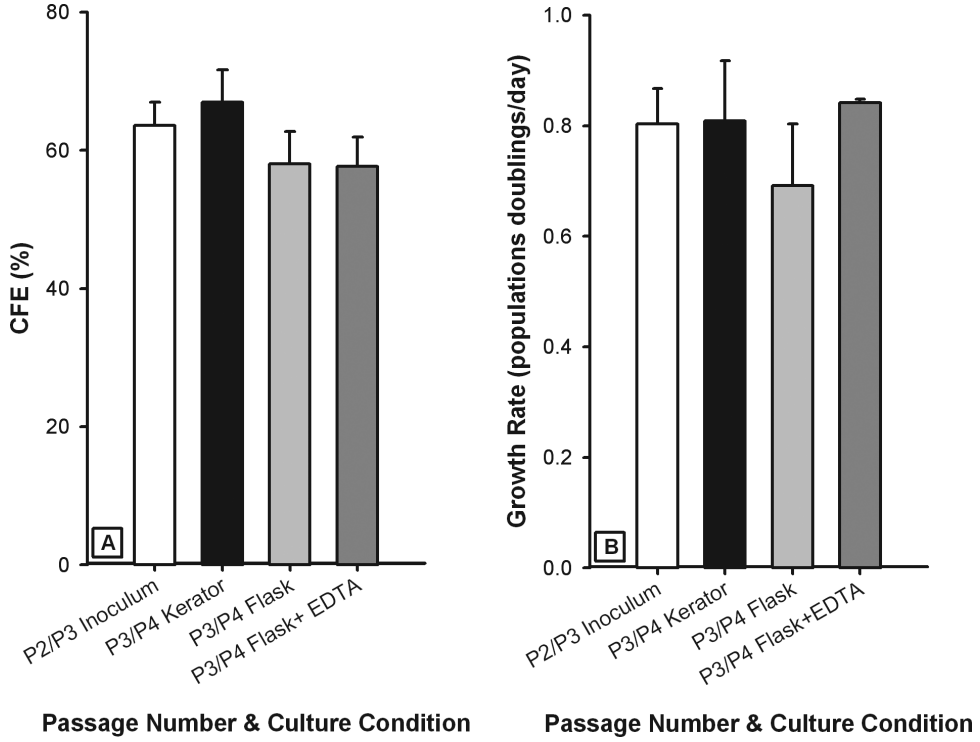

FIG. 5. CFE (%) and growth rate (PD/day) of keratinocytes at the time of inoculation into Kerator (P2/P3 inoculum), after harvest from the Kerator (P3/P4 Kerator), flasks without pretreatment with 0.02% EDTA (P3/P4 Flask), or from flasks after pretreatment with 0.02% EDTA prior to trypsinization (P3/P4 Flask + EDTA). There were no significant differences among the conditions when analyzed by one-way RM ANOVA. Error bars represent SEM.

harvested from flasks and flasks + EDTA were $58 \pm 4.7\%$ and $57.7 \pm 4.2\%$, respectively. The growth rate of keratinocytes harvested from the Kerator, in PD per day, was 0.80 ± 0.06 (Fig. 5B). The PD/day of keratinocytes harvested from flasks and flasks + EDTA were 0.69 ± 0.11 and 0.84 ± 0.01, respectively. There were no significant differences in CFE and PD/day among the conditions.

Quality analysis of ESS in vitro

Histology. ESS fabricated with keratinocytes harvested from the Kerator showed histological organization similar to ESS fabricated with keratinocytes harvested from flasks and flasks + EDTA (Fig. 6). In all three conditions, there was an epidermal substitute composed of keratinocytes attached to a dermal substitute composed of collagen sponge populated with fibroblasts.

MTT assay. MTT assay was performed on samples of ESS on days 7, 14, and 21 of maturation. There were no significant differences among the conditions at each time point (Fig. 7).

Surface electrical capacitance. Epidermal barrier property of ESS was assessed by measurement of surface hydration on days 7, 11, 14, and 21 of maturation *in vitro*. In all conditions, the SEC values of ESS decreased significantly with increasing time of maturation (Fig. 8). There were no significant differences in SEC among the three conditions at parallel time points.

DISCUSSION

Data presented in this report demonstrate advantages of the Kerator over tissue-culture flasks. These are (1) a modular growth chamber made of resterilizable material, (2) automated fluid handling during medium changes, (3) integrated video microscopy, and (4) semi-automated harvesting of sub-confluent keratinocytes while maintaining their growth potential in the subsequent passage. These advantages contribute to (1) reduced materials involved in keratinocyte expansion, (2) decreased handling of cells during culture, (3) visualization and monitoring of cultures in real time, and (4) maintenance of ESS quality for grafting. The ability to control the frequency of medium changes and environmental parameters such as temperature and CO_2 concentration in the Kerator also has important implications for regulating the physiology of proliferating keratinocytes and, therefore, of the resultant ESS.

Fluid handling during medium changes in the Kerator, including the frequency of medium changes, draining used medium, adding adequate volume of fresh medium per change, and rocking the platform to ensure even distribution of

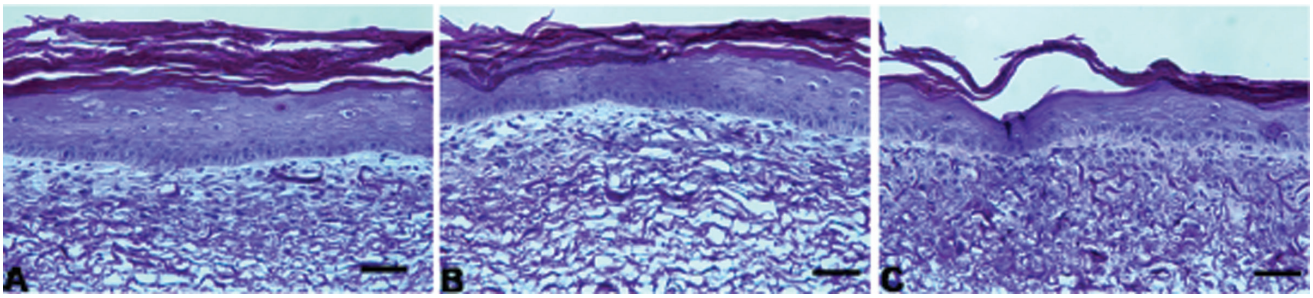

FIG. 6. H&E-stained sections of ESS after 14 days of maturation *in vitro*. ESS were fabricated with keratinocytes harvested from (**A**) Kerator, (**B**) Flasks, and (**C**) Flasks + EDTA. In all conditions, the ESS is composed of an epidermal layer of keratinocytes overlying a fibroblast-populated collagen sponge. Scale bar = 100 μm. Color images available online at www.liebertpub.com/ten.

medium within the growth chamber, was performed accurately and reproducibly in an automated manner from the point of cell inoculation by a custom LabVIEW 6.1 VI. Keratinocyte harvest from the Kerator was performed in a semi-automated manner with the growth chamber *in situ*. The image acquisition system was used during culture to assess confluence and during harvest to monitor progression of cell detachment before collection. *In situ* video microscopy and subsequent image analysis are sensitive tools for noninvasive monitoring and quantization of cell proliferation in culture.[33,34] Comparison of keratinocyte proliferation in the Kerator and standard tissue-culture flasks was performed by analysis of digital

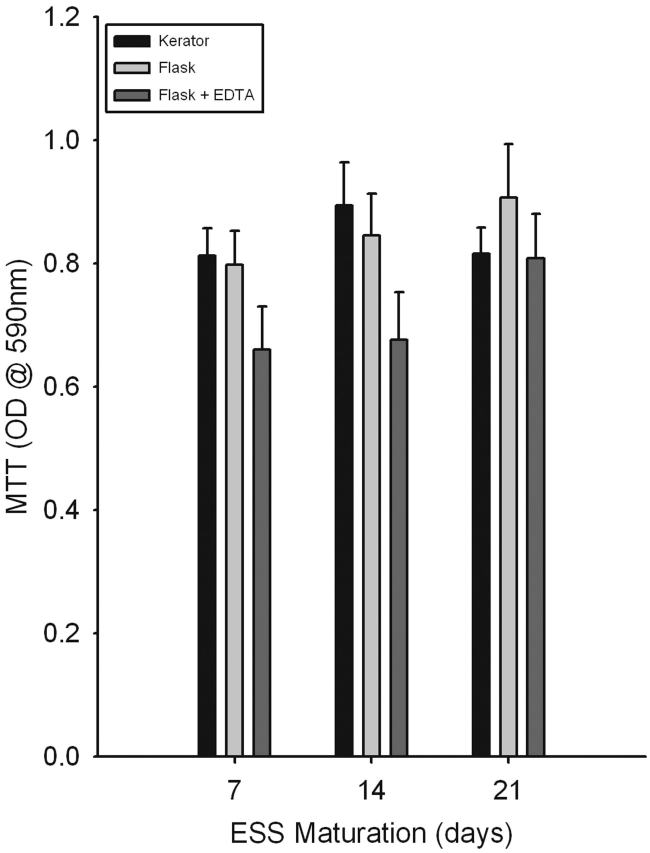

FIG. 7. MTT assay to quantify cell viability in ESS fabricated with keratinocytes harvested from the Kerator, from flasks without 0.02% EDTA pretreatment (Flask), and from flasks with 0.02% EDTA pretreatment prior to trypsinization (Flask + EDTA). There were no significant differences among the conditions when analyzed by one-way RM ANOVA. Error bars represent SEM. OD = Optical Density.

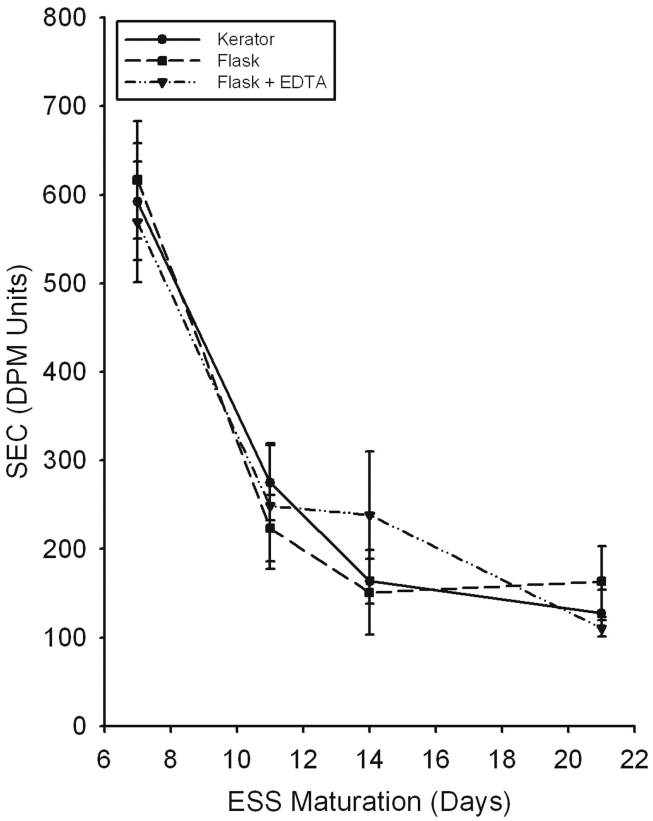

FIG. 8. The epidermal barrier in ESS fabricated with keratinocytes harvested from the Kerator, from flasks without 0.02% EDTA pretreatment (Flask), and from flasks with 0.02% EDTA pretreatment prior to trypsinization (Flask + EDTA), as evaluated by SEC. There were no significant differences among the conditions when analyzed by one-way RM ANOVA. Error bars represent SEM.

images for the extent of confluence. The images from both conditions were taken following medium changes on days 2, 4, and 6 of culture. This procedure was adopted to exclude the cells that were detached and were floating in the medium prior to medium change. In both Kerator and flasks, exponential growth of cells was obtained, but the average confluence of keratinocytes in the Kerator was less than that in flasks at day 4 of culture. We believe that this initial lag in keratinocyte confluence in the Kerator may be due to a minimal loss of cells in the tubing during transport at the time of cell seeding. However, there was no difference in confluence between the Kerator and flasks prior to harvest. This is a significant finding because it suggests that the Kerator can support keratinocyte growth to the same extent as tissue-culture flasks. This finding also agrees with that of Kino-Oka and Prenosil,[25] who found comparable rates of keratinocyte growth among the polystyrene surface of T-flasks and the FEP surface of Petriperm dishes.

The image acquisition system of the Kerator has certain strengths and limitations. The camera system offers real time collection of images with integrated image analysis to quantify cell growth. However, because the objective lens is closer to the inlet than to the outlet of the growth chamber and moves along a single horizontal axis, the images acquired might not accurately reflect keratinocyte confluence over the entire growth chamber. To correct for this limitation, it was ensured that the growth chamber was level prior to the start of culture. Also, the growth chamber was manually rocked after keratinocyte inoculation to ensure equal cell distribution across entire culture surface of the reactor chamber. As part of the preliminary studies, qualitative visual inspection of keratinocyte colonies on the culture surface of the Kerator was done after fixation with 2% glutaraldehyde and staining with 0.01% crystal violet. These studies demonstrated uniform distribution of cells along the length and breadth of the reactor chamber. Future design changes in the Kerator, such as addition of a second perpendicular axis for the movement of the objective lens, could eliminate the potential limitation due to camera location. Another limitation of the image acquisition system is that only the lowest layer of the growth chamber can be viewed by the camera. This limitation also exists in large-scale, manual cell-culture systems such as the Cell Factory. However, under the current setup of the Kerator, where each layer of the growth chamber is connected in parallel to the cell-seeding and medium conduits, it can be safely assumed that all layers receive equal volumes of the cell suspension for inoculation and hence have similar inoculation densities as the lowest layer.

The ability of FEP polymer substrate to support keratinocyte attachment and proliferation in the Kerator deserves mention. Native FEP is a hydrophobic polymer, and therefore cells do not attach to its surface. However, cells can attach and proliferate if the surface of FEP is made hydrophilic by chemical modification.[35,36] The FEP film used in the Kerator (FEP C-20) has a proprietary surface treatment in order to make it cementable. It is likely that this treatment also confers hydrophilic properties to the polymer, which enables it to support keratinocyte attachment and proliferation.

Maintenance of clonogenic potential of keratinocytes after harvest and at the time of inoculation on fibroblast-inoculated collagen sponge is essential for the formation of an epidermal layer in ESS.[37] A protocol was designed for harvesting keratinocytes from the Kerator by pretreatment with 0.02% EDTA prior to trypsinization. EDTA chelates divalent cations such as calcium and magnesium and thereby loosens the integrin-mediated attachment of keratinocytes to the culture substrate.[38] This action of EDTA reduces the time required for trypsin to detach the cells from the culture substrate. It also obviates the requirement of mechanical forces to release cells from the culture surface, following trypsinization. Keratinocytes harvested from the Kerator using this method exhibited CFE and growth rates comparable to keratinocytes harvested from tissue-culture flasks either with or without pretreatment with 0.02% EDTA. While there is a benefit of harvesting keratinocytes by pretreatment with 0.02% EDTA prior to trypsinization in the Kerator, there is no such benefit in tissue-culture flasks. This could be due to the greater hydrophilicity of FEP substrate compared to tissue-culture polystyrene, resulting in greater keratinocyte adhesion to the former.[26] The CFE and growth rates of adult-derived epidermal keratinocytes reported in this study also agree well with those reported earlier in the literature, where MCDB 153 was used as the culture medium.[30,39]

ESS fabricated with keratinocytes harvested from the Kerator showed histological organization similar to those fabricated with keratinocytes harvested from flasks. An increase in keratinization of the epidermal layer with time was observed in all conditions (data not shown), which resulted in a corresponding decrease in surface hydration by SEC. Cellular viability in ESS was comparable among the Kerator and flasks, as suggested by MTT conversion data. Studies are being undertaken to quantify the proliferating fraction of keratinocytes in ESS, by bromodeoxyuridine (BrdU) labeling during the second week of maturation *in vitro*.

This study provides evidence that epidermal keratinocytes, cultured in and harvested from an automated bioreactor, can successfully constitute well-organized and viable engineered tissue that forms epithelial barrier *in vitro*. Although keratinocytes grown on gelatin microcarriers in a bioreactor were shown to heal cutaneous wounds, this method did not entail harvesting of keratinocytes and the formation of a tissue-engineered device *in vitro* prior to transplantation.[40] Transplantation to full-thickness wounds on athymic mice of ESS fabricated with keratinocytes harvested from the Kerator is currently being undertaken to assess their capacity for wound healing *in vivo*.

In this study, we have successfully tested the potential of automating certain steps of keratinocyte culture and harvest in the Kerator for tissue engineering of ESS. Studies will be conducted in the future to fully automate the process. Although not tested in this study, medium changes in the

bioreactor could be regulated by monitoring a limiting threshold of metabolites (e.g., glucose, urea, lactate, glutamine), and this could allow more precise regulation of the physiology of cell populations.[41] Other tissue-specific cells, such as fibroblasts, endothelial cells, and melanocytes, can be similarly cultured and harvested for large-scale production of ESS. Complete automation of ESS fabrication will also require automated inoculation of cells on the polymer substrate and automated medium changes for the maturing skin substitute. A closed bioreactor system that incorporates automated scaffold seeding and perfusion culture of engineered skin has recently been described.[42] Inkjet printing of cells is an emerging technology for automated cell seeding on scaffolds.[43] Although the integration of these technologies will increase the engineering complexity of the manufacturing process, it may improve the anatomy and physiology of the tissue-engineered medical product, reduce fabrication costs, and increase product availability to the patient.

ACKNOWLEDGMENTS

The authors express their gratitude to Jodi Miller for providing cell-culture media and to Chris Lloyd for fabrication of collagen sponges. This project was supported by a research grant from the National Institutes of Health (GM050509).

REFERENCES

1. Martin, I., Wendt, D., and Heberer, M. The role of bioreactors in tissue engineering. Trends Biotechnol. **22,** 80, 2004.
2. Boudreault, P., Tremblay, J.P., Pepin, M.F., and Garnier, A. Scale-up of a myoblast culture process. J. Biotechnol. **91,** 63, 2001.
3. Gilbertson, J.A., Sen, A., Behie, L.A., and Kallos, M.S. Scaled-up production of mammalian neural precursor cell aggregates in computer-controlled suspension bioreactors. Biotechnol. Bioeng. **94,** 783, 2006.
4. Kino-Oka, M., Ogawa, N., Umegaki, R., and Taya, M. Bioreactor design for successive culture of anchorage-dependent cells operated in an automated manner. Tissue Eng. **11,** 535, 2005.
5. Liu, J.Y., Hafner, J., Dragieva, G., and Burg, G. Bioreactor microcarrier cell culture system (Bio-MCCS) for large-scale production of autologous melanocytes. Cell Transplant. **13,** 809, 2004.
6. Monga, S.P., Hout, M.S., Baun, M.J., Micsenyi, A., Muller, P., Tummalapalli, L., Ranade, A.R., Luo, J.H., Strom, S.C., and Gerlach, J.C. Mouse fetal liver cells in artificial capillary beds in three-dimensional four-compartment bioreactors. Am. J. Pathol. **167,** 1279, 2005.
7. Youn, B.S., Sen, A., Kallos, M.S., Behie, L.A., Girgis-Gabardo, A., Kurpios, N., Barcelon, M., and Hassell, J.A. Large-scale expansion of mammary epithelial stem cell aggregates in suspension bioreactors. Biotechnol. Prog. **21,** 984, 2005.
8. Chen, H.C., Lee, H.P., Sung, M.L., Liao, C.J., and Hu, Y.C. A novel rotating-shaft bioreactor for two-phase cultivation of tissue-engineered cartilage. Biotechnol. Prog. **20,** 1802, 2004.
9. Janssen, F.W., Oostra, J., Oorschot, A., and van Blitterswijk, C.A. A perfusion bioreactor system capable of producing clinically relevant volumes of tissue-engineered bone: *in vivo* bone formation showing proof of concept. Biomaterials **27,** 315, 2006.
10. Mahmoudifar, N., and Doran, P.M. Tissue engineering of human cartilage in bioreactors using single and composite cell-seeded scaffolds. Biotechnol. Bioeng. **91,** 338, 2005.
11. Song, K., Yang, Z., Liu, T., Zhi, W., Li, X., Deng, L., Cui, Z., and Ma, X. Fabrication and detection of tissue-engineered bones with bio-derived scaffolds in a rotating bioreactor. Biotechnol. Appl. Biochem. **45,** 65, 2006.
12. Williams, C., and Wick, T.M. Perfusion bioreactor for small diameter tissue-engineered arteries. Tissue Eng. **10,** 930, 2004.
13. Jeong, S.I., Kwon, J.H., Lim, J.I., Cho, S.W., Jung, Y., Sung, W.J., Kim, S.H., Kim, Y.H., Lee, Y.M., Kim, B.S., Choi, C.Y., and Kim, S.J. Mechano-active tissue engineering of vascular smooth muscle using pulsatile perfusion bioreactors and elastic PLCL scaffolds. Biomaterials **26,** 1405, 2005.
14. Mol, A., Driessen, N.J., Rutten, M.C., Hoerstrup, S.P., Bouten, C.V., and Baaijens, F.P. Tissue engineering of human heart valve leaflets: a novel bioreactor for a strain-based conditioning approach. Ann. Biomed. Eng. **33,** 1778, 2005.
15. Seidel, J.O., Pei, M., Gray, M.L., Langer, R., Freed, L.E., and Vunjak-Novakovic, G. Long-term culture of tissue engineered cartilage in a perfused chamber with mechanical stimulation. Biorheology **41,** 445, 2004.
16. Saini, S., and Wick, T.M. Concentric cylinder bioreactor for production of tissue engineered cartilage: effect of seeding density and hydrodynamic loading on construct development. Biotechnol. Prog. **19,** 510, 2003.
17. Gallico, G.G., III, O'Connor, N.E., Compton, C.C., Kehinde, O., and Green, H. Permanent coverage of large burn wounds with autologous cultured human epithelium. N. Engl. J. Med. **311,** 448, 1984.
18. Godbey, W.T., and Atala, A. *In vitro* systems for tissue engineering. Ann. N.Y. Acad. Sci. **961,** 10, 2002.
19. Boyce, S.T., Kagan, R.J., Yakuboff, K.P., Meyer, N.A., Rieman, M.T., Greenhalgh, D.G., and Warden, G.D. Cultured skin substitutes reduce donor skin harvesting for closure of excised, full-thickness burns. Ann. Surg. **235,** 269, 2002.
20. Boyce, S.T., Kagan, R.J., Greenhalgh, D.G., Warner, P., Yakuboff, K.P., Palmieri, T., and Warden, G.D. Cultured skin substitutes reduce requirements for harvesting of skin autograft for closure of excised, full-thickness burns. J. Trauma **60,** 821, 2006.
21. Passaretti, D., Billmire, D., Kagan, R., Corcoran, J., and Boyce, S. Autologous cultured skin substitutes conserve donor autograft in elective treatment of congenital giant melanocytic nevus. Plast. Reconstr. Surg. **114,** 1523, 2004.
22. Vailly, J., Gagnoux-Palacios, L., Dell'Ambra, E., Romero, C., Pinola, M., Zambruno, G., De, L.M., Ortonne, J.P., and Meneguzzi, G. Corrective gene transfer of keratinocytes from patients with junctional epidermolysis bullosa restores assembly of hemidesmosomes in reconstructed epithelia. Gene Ther. **5,** 1322, 1998.
23. White, S.J., Page, S.M., Margaritis, P., and Brownlee, G.G. Long-term expression of human clotting factor IX from

retrovirally transduced primary human keratinocytes *in vivo*. Hum. Gene Ther. **9,** 1187, 1998.
24. Boyce, S.T., and Warden, G.D. Principles and practices for treatment of cutaneous wounds with cultured skin substitutes. Am. J. Surg. **183,** 445, 2002.
25. Kino-Oka, M., and Prenosil, J.E. Development of an on-line monitoring system of human keratinocyte growth by image analysis and its application to bioreactor culture. Biotechnol. Bioeng. **67,** 234, 2000.
26. Kino-Oka, M., and Prenosil, J.E. Growth of human keratinocytes on hydrophilic film support and application to bioreactor culture. J. Chem. Eng. Jpn. **31,** 856, 1998.
27. Prenosil, J.E., and Villeneuve, P.E. Automated production of cultured epidermal autografts and sub-confluent epidermal autografts in a computer controlled bioreactor. Biotechnol. Bioeng. **59,** 679, 1998.
28. Prenosil, J.E., and Kino-Oka, M. Computer controlled bioreactor for large-scale production of cultured skin grafts. Ann. N.Y. Acad. Sci. **875,** 386, 1999.
29. Bishop, R.H. Learning with LabVIEW 6i. Upper Saddle River, NJ: Prentice Hall, 2001.
30. Boyce, S.T., and Ham, R.G. Calcium-regulated differentiation of normal human epidermal keratinocytes in chemically defined clonal culture and serum-free serial culture. J. Invest. Dermatol. **81,** 33s, 1983.
31. Boyce, S.T., Supp, A.P., Swope, V.B., and Warden, G.D. Vitamin C regulates keratinocyte viability, epidermal barrier, and basement membrane *in vitro*, and reduces wound contraction after grafting of cultured skin substitutes. J. Invest. Dermatol. **118,** 565, 2002.
32. Boyce, S.T., Supp, A.P., Harriger, M.D., Pickens, W.L., Wickett, R.R., and Hoath, S.B. Surface electrical capacitance as a noninvasive index of epidermal barrier in cultured skin substitutes in athymic mice. J. Invest. Dermatol. **107,** 82, 1996.
33. Perricone, M.A., Saldate, V., and Hyde, D.M. Quantitation of fibroblast population growth rate *in situ* using computerized image analysis. Microsc. Res. Tech. **31,** 257, 1995.
34. Teague, T.K., Munn, L., Zygourakis, K., and McIntyre, B.W. Analysis of lymphocyte activation and proliferation by video microscopy and digital imaging. Cytometry **14,** 772, 1993.
35. Steele, J.G., Johnson, G., McFarland, C., Dalton, B.A., Gengenbach, T.R., Chatelier, R.C., Underwood, P.A., and Griesser, H.J. Roles of serum vitronectin and fibronectin in initial attachment of human vein endothelial cells and dermal fibroblasts on oxygen- and nitrogen-containing surfaces made by radiofrequency plasmas. J. Biomater. Sci. Polym. Ed. **6,** 511, 1994.
36. Steele, J.G., Johnson, G., Griesser, H.J., and Underwood, P.A. Mechanism of initial attachment of corneal epithelial cells to polymeric surfaces. Biomaterials **18,** 1541, 1997.
37. Green, H., Kehinde, O., and Thomas, J. Growth of cultured human epidermal cells into multiple epithelia suitable for grafting. Proc. Natl. Acad. Sci. U.S.A. **76,** 5665, 1979.
38. Lange, T.S., Bielinsky, A.K., Kirchberg, K., Bank, I., Herrmann, K., Krieg, T., and Scharffetter-Kochanek, K. Mg^{2+} and Ca^{2+} differentially regulate beta 1 integrin-mediated adhesion of dermal fibroblasts and keratinocytes to various extracellular matrix proteins. Exp. Cell Res. **214,** 381, 1994.
39. Wille, J.J., Jr., Pittelkow, M.R., Shipley, G.D., and Scott, R.E. Integrated control of growth and differentiation of normal human prokeratinocytes cultured in serum-free medium: clonal analyses, growth kinetics, and cell cycle studies. J. Cell Physiol. **121,** 31, 1984.
40. Liu, J.Y., Hafner, J., Dragieva, G., Seifert, B., and Burg, G. Autologous cultured keratinocytes on porcine gelatin microbeads effectively heal chronic venous leg ulcers. Wound Repair Regen. **12,** 148, 2004.
41. Chee Furng, W.D., Tin Kam, W.K., Tang, G.L., Kiat, H.C., and Gek Sim, Y.M. Impact of dynamic online fed-batch strategies on metabolism, productivity and N-glycosylation quality in CHO cell cultures. Biotechnol. Bioeng. **89,** 164, 2005.
42. Sun, T., Norton, D., Haycock, J.W., Ryan, A.J., and MacNeil, S. Development of a closed bioreactor system for culture of tissue-engineered skin at an air-liquid interface. Tissue Eng. **11,** 1824, 2005.
43. Xu, T., Jin, J., Gregory, C., Hickman, J.J., and Boland, T. Inkjet printing of viable mammalian cells. Biomaterials **26,** 93, 2005.

Address reprint requests to:
Steven Boyce, Ph.D.
Shriners Burns Hospital
3229 Burnet Avenue
Cincinnati, OH 45229

E-mail: boycest@uc.edu